

Jian-Lian Chen  
Te-Ling Lu  
Yi-Chen Lin

School of Pharmacy, China  
Medical University, Taichung,  
Taiwan

Received April 16, 2010

Revised June 6, 2010

Accepted June 7, 2010

## Research Article

# Multi-walled carbon nanotube composites with polyacrylate prepared for open-tubular capillary electrochromatography

A new phase containing immobilized carbon nanotubes (CNTs) was synthesized by *in situ* polymerization of acid-treated multi-walled CNTs using butylmethacrylate (BMA) as the monomer and ethylene dimethacrylate as the crosslinker on a silanized capillary, forming a porous-layered open-tubular column for CEC. Incorporation of CNT nanomaterials into a polymer matrix could increase the phase ratio and take advantage of the easy preparation of an OT-CEC column. The completed BMA-CNT column was characterized by SEM, ATR-IR, and EOF measurements, varying the pH and the added volume organic modifier. In the multi-walled CNTs structure, carboxylate groups were the major ionizable ligands on the phase surface exerting the EOF having electroosmotic mobility,  $4.0 \times 10^4 \text{ cm}^2 \text{ V}^{-1} \text{ S}^{-1}$ , in the phosphate buffer at pH 2.8 and RSD values ( $n = 5$ ), 3.2, 4.1, and 4.3%, for three replicate capillaries at pH 7.6. Application of the BMA-CNT column in CEC separations of various samples, including nucleobases, nucleosides, flavonoids, and phenolic acids, proved satisfactory upon optimization of the running buffers. Their optima were found in the borate buffers at pH 9.0/50 mM, pH 9.5/10 mM/50% v/v ACN, and pH 9.5/30 mM/10% v/v methanol, respectively. The separations could also be used to assess the relative contributions of electrophoresis and chromatography to the CEC mechanism by calculating the corresponding velocity and retention factors. Discussions about interactions between the probe solutes and the bonded phase included the  $\pi$ - $\pi$  interactions, electrostatic repulsion, and hydrogen bonding. Furthermore, a reversed-phase mode was discovered to be involved in the chromatographic retention.

### Keywords:

Capillary electrochromatography / Multi-wall carbon nanotube / Open-tubular / Polyacrylate / Porous layer  
DOI 10.1002/elps.201000226

## 1 Introduction

The stationary phases in CEC and/or capillary liquid chromatography have been extensively developed to meet the demands of microscale separations. When considering a novel stationary phase for some specific application, a proper method of coating the phase onto the column should also be taken into account to ensure that the phase design is practical. Among the column formats, the open-tubular

(OT) style is comparatively straightforward; it does not require the fabrication of any frits to retain particulate packing or the precise blending of monomeric reagents with suitable porogens, as is required for monoliths [1, 2]. However, OT-CEC suffers from a low-phase ratio of available functional ligands attached to the capillary wall. Methods generally used to increase the loadability of phase materials include etching the capillary wall, stacking with multilayers, or coating the capillary with porous polymeric layers [3–5]. These strategies are achieved either by physical coating of functional moieties on the column or by chemical bonding. Due to concerns about the column lifetime and reproducibility, it is better if the OT-CEC capillaries are modified with covalently attached ligands. Modified capillaries can be produced by the sol-gel approach [6], by stepwise fabrication (usually starting with a silanized capillary) [7], by direct coating with polymers [8], or by the *in situ* polymerization of functional monomers [9].

Nanoparticles exhibiting favorable surface-to-volume ratios can be efficient stationary phases for CEC [10]. Some

**Correspondence:** Dr. Jian-Lian Chen, School of Pharmacy, China Medical University, No. 91 Hsueh-Shih Road, Taichung 40402, Taiwan

**E-mail:** cjl@mail.cmu.edu.tw

**Fax:** +886-4-22031075

**Abbreviations:** **Ade**, adenine; **Ado**, adenosine; **BMA**, butylmethacrylate; **CNT**, carbon nanotube; **Cyd**, cytidine; **Cyt**, cytosine; **Gua**, guanine; **Guo**, guanosine; **MeOH**, methanol; **MWNT**, multi-walled carbon nanotube; **PLOT**, porous-layered open-tubular; **Thd**, thymidine; **Thy**, thymine; **Ura**, uracil; **Urd**, uridine

nanomaterials, including latex [11], lipoprotein [12, 13], silica [14, 15], titanium oxide [16, 17], gold [18–20], and carbon nanotubes (CNT) [21–25], have been used in OT-CEC. However, only a few examples involved in chemical bonding of these materials onto OT capillaries exist. Among the immobilization methods, high-temperature dehydration was only desirable for particles with wholly inorganic compositions [15–17]. Silanization was a useful alternative for particles that could degrade at high-reaction temperatures [18, 19, 24]. In our previous paper, the CNT materials were designed to attach to the silica hydride modified phase by forming a stable covalent Si-C bond [25]. Until now, there have been no reports on the attachment of CNT onto capillaries through *in situ* polymerization, except for the simple synthesis of CNT/polyacrylate composites [26, 27].

Our previous results showed the superiority of *in situ* polymerization over the stepwise fabrication starting with a silica hydride capillary and the same acrylate ligands on an OT-CEC column [28]. The *in situ* approach forms a porous polymeric layer with more functional ligands loaded on the column than the stepwise approach, which only affords a monolayered phase. The fabrication of a porous-layer open-tubular (PLOT) capillary is much easier than making a monolith and is suitable for pioneering studies of new stationary phases. Although there is still concern about the low-phase ratios, researchers have demonstrated the separation of various analytes on styrene-based [29], acrylate-based [30], and styrene-acrylate-based [31] PLOT columns.

This study explores *in situ* polymerization of CNTs immobilized in a PLOT format. Carbon-atom pentagons at the curvature points in the CNTs are assumed to be involved in the  $\pi$ -bonds that break during the polymerization reaction [26, 27]. The carboxylated multi-walled carbon nanotubes (MWNTs) were copolymerized with butylmethacrylate (BMA) monomer and ethylene dimethacrylate crosslinker on a silanized capillary. The complete BMA-CNT PLOT column was characterized by the measurements of SEM, ATR-IR, and electroosmotic mobilities ( $\mu_{\text{eo}}$ ) based on the changes of buffer conditions. Samples of nucleobases, nucleosides, flavonoids, and phenolic acids were used to test the OT-CEC separations. In addition, the discrimination between electrophoretic and chromatographic contribution to the CEC mechanism was examined for these separations.

## 2 Materials and methods

### 2.1 Reagents and chemicals

Most chemicals used were of analytical or chromatographic grade. Purified water (18 M $\Omega$ cm) from a Milli-Q water purification system (Millipore, Bedford, MA, USA) was used to prepare samples and buffer solutions. All the solvents and solutions for the CEC analysis were filtered through a 0.45  $\mu\text{m}$  cellulose ester membrane (Advantec MFS, Pleasanton, CA, USA).

### 2.1.1 Reagents

Ethylene dimethacrylate, 2,2-diphenyl-1-picrylhydrazyl, 2,2'-azo-bis-isobutyronitrile, sodium tetraborate, phosphoric acid, hydrochloric acid, ACN, 1,4-butanediol, and DMSO were purchased from Sigma-Aldrich (Milwaukee, WI, USA). Boric acid, tri-sodium phosphate, methanol (MeOH), acetone, and ethanol were obtained from Panreac (Barcelona, Spain). BMA, nitric acid, sodium hydroxide, sodium dihydrogenphosphate, disodium hydrogenphosphate, tri-sodium phosphate, ammonium carbonate, ammonium hydroxide, and 1-propanol were supplied by Merck KGaA (Garmstadt, Germany). 3-(Trimethoxysilyl) propylmethacrylate ( $\gamma$ -MAPS) was received from Acros (Thermo Fisher Scientific, Geel, Belgium).

The MWNT materials were supplied by Conyuan Biochemical Technology (Taipei, Taiwan) and their specifications are: 20–40 nm for the external diameter, 5–15  $\mu\text{m}$  length, 95–98% purity, by volume, 40–300 m<sup>2</sup>/g for the special surface area, 2 wt% amorphous carbon, and 0.2 wt% of ash.

### 2.1.2 Analytes

Nucleobases (thymine (Thy), cytosine (Cyt), adenine (Ade), guanine (Gua), uracil (Ura)); nucleosides (thymidine (Thd), cytidine (Cyd), adenosine (Ado), guanosine (Guo), uridine (Urd)); flavonoids (5-methoxyflavone, hesperidin, naringin, epicatechin, hesperetin, daidzein, naringenin, and quercetin); phenolic acids (chlorogenic, *p*-coumaric, gallic, ferulic, caffeic, and protocatechuic acids); and ethylvanillin were purchased from Sigma-Aldrich. Syringic acid and vanillic acid were received from Acros (Thermo Fisher Scientific). *p*-Hydroxybenzoic acid was obtained from Merck KGaA.

To make stock sample solutions, nucleobases and nucleosides were dissolved in H<sub>2</sub>O (each 0.2 mg/mL), flavonoids were dissolved in MeOH (each 0.25 mg/mL, except for epicatechin, hesperetin, and naringenin, 0.5 mg/mL), and phenolic acids were dissolved in H<sub>2</sub>O (0.1 M). The test samples were collected from stock solutions with equal volume.

## 2.2 Apparatus

The laboratory-built electrophoresis apparatus consisted of a  $\pm 30$  kV high-voltage power supply (TriSep TM-2100, Unimicro Technologies, CA, USA) and a UV-Vis detector (LCD 2083.2 CE, ECOM, Prague, Czech). Electrochromatograms were recorded using a Peak-ABC Chromatography Data Handling System (Kingtech Scientific, Taiwan). The SEM images were acquired at an accelerating voltage of 3.0 kV by a Joel JSM-6700F Scanning Microscopy at National Chung Hsing University. The ATR-IR spectra were obtained by a Shimadzu Prestige-21 IR spectrometer, equipped with a single reflection horizontal ATR accessory (MIRacle, PIKE Technologies, WI, USA).

### 2.3 Preparation of capillary columns

A new, bare capillary column (Polymicro Technologies, Phoenix, AZ, USA) with 375  $\mu\text{m}$  od  $\times$  75  $\mu\text{m}$  id was treated with 1.0 M NaOH and successively washed with pure water, 1.0 M HCl, pure water, and acetone. The clean, bare capillary was then filled with a solution of 2,2-diphenyl-1-picrylhydrazyl (0.02 g),  $\gamma$ -MAPS (1.0 mL), and MeOH (1.0 mL) and was kept at room temperature for 24 h to complete silanization. After rinsing with MeOH, H<sub>2</sub>O, and acetone, the resulting silanized capillary was filled with a monomer solution, which contained BMA (0.03 mol), ethylene dimethacrylate (0.01 mol), acid-treated MWNTs (1 mg), 2,2'-azo-bis-isobutyronitrile (0.1 g), 1-propanol (4.5 mL), 1,4-butanediol (4.5 mL), and H<sub>2</sub>O (1 mL). The acid-treated MWNTs were obtained by first refluxing the MWNTs with HNO<sub>3</sub> (3.0 M) for 24 h at 60°C and, then, with HCl (5.0 M) for 6 h at 120°C. After standing for 1 h at ambient temperature, the mixture was purged *via* the application of a nitrogen flow at 15 psi for 1 h, leaving a thin layer of monomer material ready to react with the silanized capillary. The capillaries were sealed at both ends and heated in an oven at 70°C for 24 h to complete the polymerization reaction. Finally, the completed BMA-CNT capillaries were washed successively with H<sub>2</sub>O, 1-propanol, and acetone for 30 min and were then prepared for the CEC experiments.

### 2.4 CEC conditions

The BGE used was ammonium carbonate, sodium phosphate, and sodium borate buffer; DMSO was used as the neutral marker. At the end of analysis, the studied capillary was washed with methanol, pure water, and running buffer sequentially during the intervals between runs. Prior to a sample injection, a working voltage was applied for 5 min to condition the charge distribution in the column. The samples were introduced by siphoning using a height difference and were detected by UV light absorption measurement at 214 nm for DMSO, 254 nm for nucleobases and nucleosides, and 280 nm for flavonoids and phenolic acids.

## 3 Results and discussion

### 3.1 Characterization of BMA-CNT phase

#### 3.1.1 ATR-IR spectrum and SEM image

The ATR-IR spectra of the finely ground powders of the MWNT material, the BMA-CNT bulk material, and the BMA-CNT capillary are shown in Fig. 1(A–C), respectively. All these substances present the characteristic absorption of CNTs at 1520  $\text{cm}^{-1}$  for conjugated C = C stretching [32], 1640  $\text{cm}^{-1}$  for the non-conjugated C = C stretching [33], 1700  $\text{cm}^{-1}$  for C = O stretching [33, 34] and around

3500  $\text{cm}^{-1}$  for –OH stretching [35] from the carboxyl groups introduced by the HNO<sub>3</sub>/HCl treatment of MWNTs. Carboxyl groups are reported to be the major product of nitric acid oxidation of CNTs [36], although the oxidation reaction might produce other oxygen containing functional groups as reported for some carbon materials [37].

Compared to the spectrum of acid-treated MWNTs, the spectrum of BMA-CNT shows a higher absorption ratio of C = O stretching at 1700  $\text{cm}^{-1}$  to conjugated C = C stretching at 1520  $\text{cm}^{-1}$ . The increase in C = O absorption was due to the graft of acrylate onto the MWNTs, where Fig. 2(A) shows the SEM image of the polymer composites. Figure 2(B) presents the SEM image of the BMA-CNT composite coated on the silanized capillary by means of the *in situ* polymerization process. Here the image shows the morphology at the capillary wall rim, where some polymer collapsed while cutting the capillary sample. The two circled images in Fig. 2(B) reveal some of the embedded MWNTs obviously appearing in the collapsed polymers and the remainings near the capillary rim. After attachment to the capillary, the Si-O stretching corresponding to the capillary material appeared at 1100  $\text{cm}^{-1}$  as shown in Fig. 1(C).

#### 3.1.2 EOF profiles at buffer pH

Before applying the BMA-CNT capillary to electrochromatographic analyses, characterization of the EOF driven by the capillary in different media is necessary and the measurements reveal the surface properties of the BMA-CNT phase. The four curves shown in Fig. 3 illustrate the dependence of electroosmotic mobilities ( $\mu_{\text{eo}}$ ) on the pH values of the phosphate buffers for a bare, fused-silica capillary, a  $\gamma$ -MAPS silanized capillary, a BMA-CNT capillary, and a BMA-MES capillary. The curve for the BMA-MES capillary, which was prepared using succinate methacrylate (MES) monomer instead of MWNTs, was adapted from a previous study [28].

Among the curves, the  $\gamma$ -MAPS and BMA-MES capillaries showed a pattern similar to the bare capillary. The  $\gamma$ -MAPS capillary showed a nearly 20% decrease in its  $\mu_{\text{eo}}$  value, compared with the bare capillary. By definition,  $\mu_{\text{eo}}$  is proportional to zeta potential. For the SiO<sub>2</sub> surface, the zeta potential corresponds most closely to the effective diffuse layer potential in the linear Poisson-Boltzmann approximation [38]. From the electroneutrality of the double layer, the linear relationship between the diffuse layer potential ( $\psi_d$ ) and the surface charge density ( $\sigma$ ) is given by  $\psi_d = \varepsilon 4\pi\sigma (\kappa)^{-1}$ , where  $\varepsilon$  is permittivity and  $\kappa$  is the Debye parameter. The non-dissociated  $\gamma$ -MAPS molecules immobilized on the capillary could not produce any surface charge density, but silanol molecules could. That is, nearly 80% of silanol groups were still present in the capillary after silanization and were unreacted beneath the cover of the BMA-MES polyacrylates. The contribution of the unreacted silanol residues to EOF could, therefore, continue to affect the BMA-MES capillary. However, the silanol moieties seemed

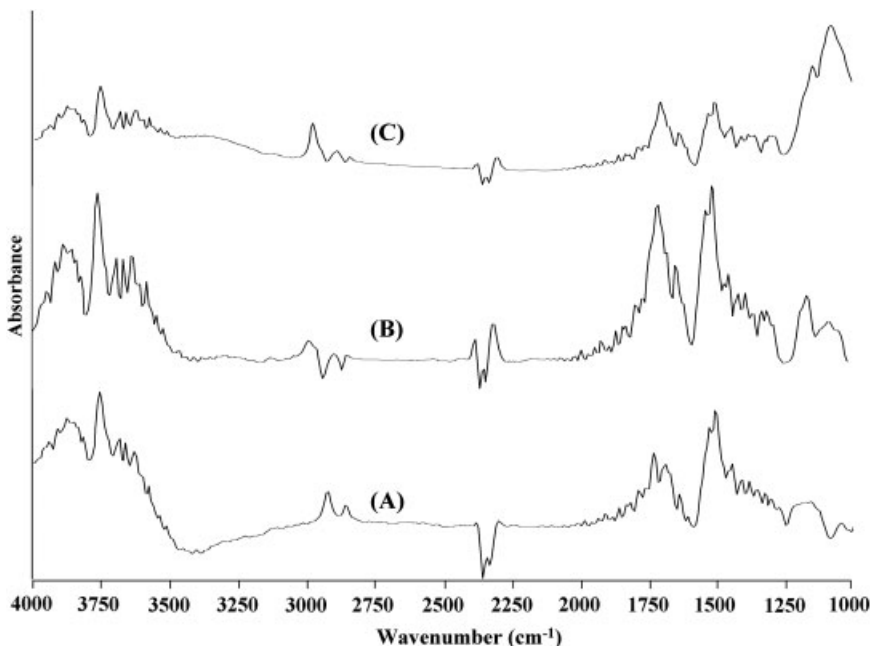


**Figure 1.** ATR-IR spectra of (A) the acid-treated multi-walled CNT, (B) the BMA-CNT as a powder, and (C) the BMA-CNT in a capillary.

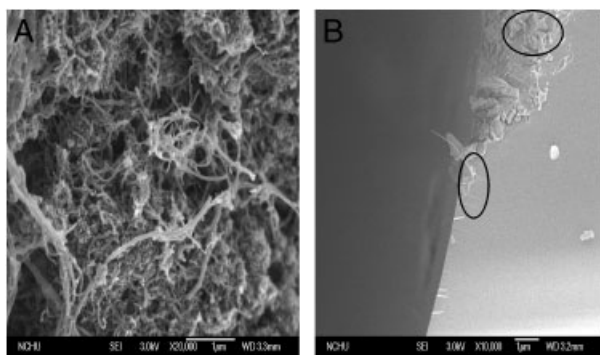


**Figure 2.** SEM images of (A) the BMA-CNT composite at 20,000 $\times$  magnification and (B) as a coating on a capillary wall, at 10,000 $\times$  magnification. The voltage used was 3.0 kV.

to be somewhat shielded by the BMA-CNT polymer and had limited impact on the EOF performance of the BMA-CNT capillary because its  $\mu_{eo}$  values did not have an obviously steep increase beginning around the pH 6.8 as observed with the other three capillaries. Instead, the curve for the BMA-CNT capillary rose smoothly along with increasing pH levels and seemed to be comprised of two lines with different slopes. The two lines intersect around pH 7.2, which correlates to the dissociation constants of the carboxylic groups on the MWNTs of the BMA-CNT matrix if the effect of silanols on the EOF is neglected. For most free carboxylic acids, their  $pK_a$  value was in the range of 3.5. An increase in the  $pK_a$  value resulting from polymerization could also be observed in polymethacrylic acid-based monoliths [39]. At pH values higher than 8.5, the dissociation of carboxylic groups in BMA-MES and BMA-CNT matrices should be complete. Here the loading of MWNTs

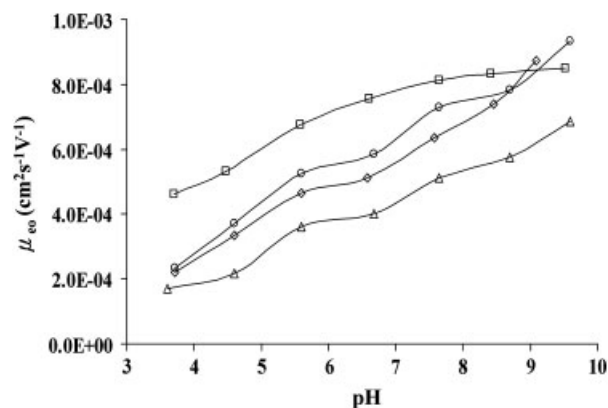


**Figure 3.** Dependence of electroosmotic mobility on buffer pH. Columns: ( $\diamond$ ) a bare silica capillary; ( $\Delta$ ) a  $\gamma$ -MAPS-silanized capillary; ( $\square$ ) the BMA-CNT capillary; ( $\circ$ ) the BMA-MES capillary, the data of which were obtained from a previous study [27]. Conditions: BGE, phosphate buffer, 50 mM; sample, DMSO; hydrostatic injection, 10 cm, 1 s; applied voltage, 15 kV; detection, 214 nm.

might be higher than MES moieties during their polymerization with BMA monomers if the contribution of residual silanols in the BMA-MES capillary to the total  $\mu_{eo}$  values is considered. With the high loading of MWNTs, the BMA-CNT capillary still kept a high-EOF velocity of  $4.0 \times 10^4 \text{ cm}^2 \text{ V}^{-1} \text{ S}^{-1}$ , even at pH 2.8.

The reproducibility of capillary fabrication was evaluated using the  $\mu_{eo}$  values measured at pH 7.6 for five trials in a BMA-CNT capillary with the same format. The RSD values were 3.2, 4.1, and 4.3% for three replicate capillaries. At the 95% confidence level, no difference between the columns has been established.

### 3.1.3 The EOF profiles upon the ratio of ACN modifier

The effect of ACN in the buffer solution on the  $\mu_{eo}$  values is highlighted in Fig. 4, which shows EOF at a minimum when ACN content is 40–60%. In fact, the concave shape of the curve could be found in various OT-CEC formats, specifically, in capillaries prepared by direct polymer coating, by stepwise fabrication, or by *in situ* polymerization [8, 28, 40, 41]. The  $\mu_{eo}$  values determined by using the neutral solute DMSO did not increase with an increasing ratio of ACN in the eluent, acting as if a reversed-phase chromatography solvent was not present at all. Apparently, these results were primarily due to a change in the ratio of dielectric constant to viscosity of the running buffer with the ACN proportion increasing from 0 to 100% (see the  $Y_2$  axis in Fig. 4). This situation suggested that the DMSO solute was a good EOF probe and its chromatographic interaction with the MWNT immobilized phases could be ignored.

### 3.2 Separations of nucleobases and nucleosides

Five nucleobases and five nucleosides were used as probes for the CEC separation performance in the BMA-CNT capillary. For both classes of samples, experiments with a series of widely used CZE buffers, namely sodium phosphate, ammonium carbonate and sodium borate, at a pH range of 8.0–10.0 and an ionic concentration range of 10–100 mM were tried. The results achieved with a borate-based buffer system showed good peak shapes and resolution in Fig. 5(A, B) for sample nucleobases and nucleosides, respectively. The satisfactory selectivity might, in part, be attributable to the formation of complexes between the borate ions and the diol groups of the ribose units linked in the nucleosides [42, 43].

Differentiating between the electrophoretic and chromatographic contributions to the CEC separation is essential, particularly in this study, which focuses on the

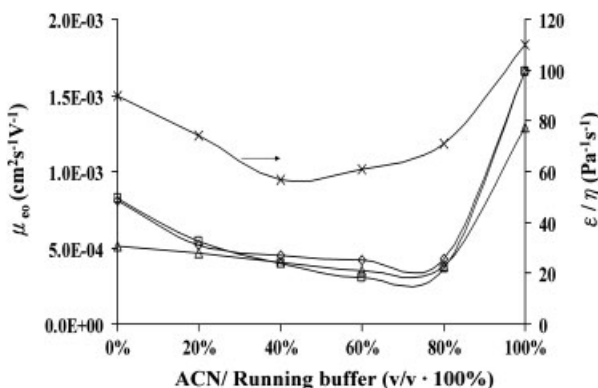


**Figure 4.** Electroosmotic mobility as a function of ACN percentage in the phosphate buffer. Conditions: BGE, mixing with phosphate buffer, pH 7.5, 10 mM, and ACN; applied voltage, 20 kV. Sample and column are the same as in Fig. 3. (x) denotes the  $\epsilon/\eta$  values of the mixing buffer.

retention induced by MWNTs. Addition of organic modifiers into the borate buffer might be an effective way to find clues to the partitioning behavior between solutes and the stationary phase. Figure 5(C, D) shows electrochromatograms for the separations of nucleobases with MeOH (10%; v/v) and nucleosides with ACN (10%; v/v), respectively. If only chromatographic retention is considered, the retention times should decrease as organic modifiers are added to the eluent. However, the migration times for each of the peaks appearing in Fig. 5(C, D) were longer than the corresponding solutes shown in Fig. 5(A, B). Here the reduced EOF resulting from the addition of organic modifiers into running buffers, as shown in Fig. 4, would interfere with the observation of retention times. Moreover, the orders of elution shown in Fig. 5 were very different from the orders obtained from bare capillaries: Thy (eluted first) > Ade > Ura > Cyt > Gua for nucleobases and Ado > Cyd > Thd > Urd > Guo for nucleosides. The BMA-CNT column might show another chromatographic mechanism in addition to electrophoresis.

Adopting the definition by Rathore and Horváth, measures of electrophoretic migration and chromatographic retention in CEC can be displayed as a velocity factor ( $k'_e$ ) and a retention factor ( $k''$ ), respectively [44, 45]. In brief, they are expressed by Eq. (1) and (2):

$$k'_e = \frac{\mu_{ep}}{\mu_{eo2}} \quad (1)$$

$$k'' = \frac{[t_M \times (1 + k'_e) - t_{02}]}{t_{02}} \quad (2)$$

where  $\mu_{ep}$  and  $\mu_{eo2}$  are the electrophoretic and electroosmotic mobility. Values for  $\mu_{ep}$  and  $\mu_{eo2}$  can be obtained, respectively, from OT CE experiments on a bare capillary (column 1) and from the CEC experiments on the MWNT immobilized capillary (column 2) as follows:

$$\mu_{ep} = \frac{L_1 \times L_{d1}}{V_1} \times \left( \frac{1}{t_{M1}} - \frac{1}{t_{01}} \right)$$

$$\mu_{eo2} = \frac{L_2 \times L_{d2}}{t_{02} \times V_2}$$

where  $L$  is the total column length,  $L_d$  is the distance between the inlet and the detection point,  $V$  is the applied voltage,  $t_M$  is the migration time of solute, and  $t_0$  is the migration time of DMSO. The electrophoretic and chromatographic migration parameters responsible for the separations using the conditions shown in Fig. 5(C, D) are collected in Table 1. The  $k'_e$  values are negative, which means that the electrophoretic migration of solutes was counter to the cathodic EOF in our buffer system. Although their  $pK_a$  values are larger than 9.0, some of the solutes migrated toward the anode under the acetate [46], carbonate [47], and borate/diethylamine buffers [43], around pH 9.0 in a CZE mode. The order of  $k'_e$  values typically correlated with the  $pK_a$  values calculated from the results of CZE (nucleobases: Thy (10.2) > Ade (10.1) > Ura (9.8) > Gua (9.8); nucleosides: Thd (10.5) > Urd (10.0) > Guo (10.0) [46]. Of

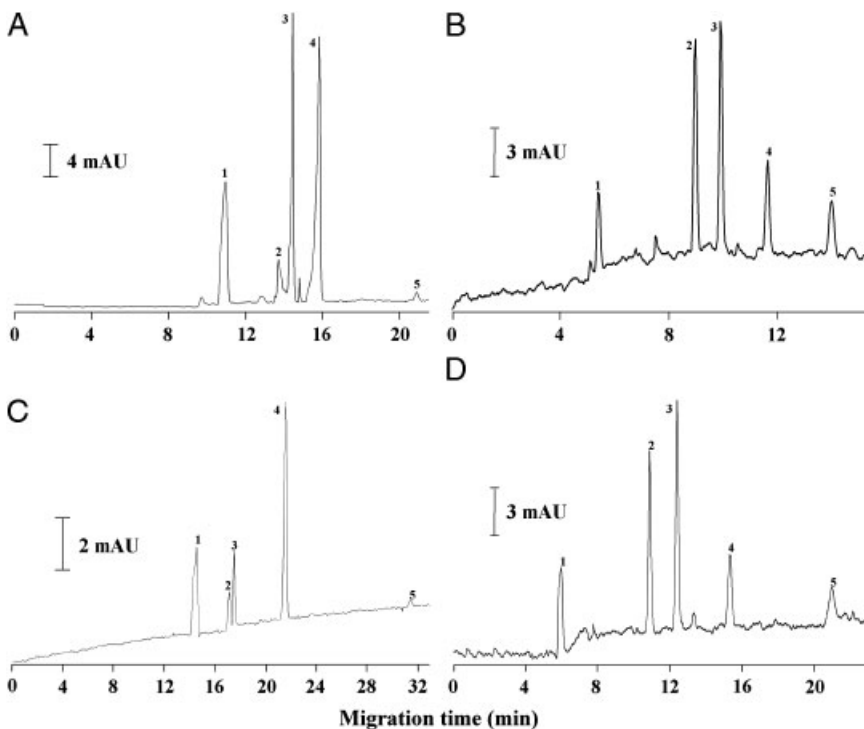


**Figure 5.** Electrochromatographic separations of nucleobases and nucleosides in the BMA-CNT capillary with and without organic modifiers added in BGE. (A) 0%; (B) 0%; (C) 10% (v/v) MeOH; (D) 10% (v/v) ACN added in the borate buffer, 50 mM, pH 9.0. Applied voltage: 12 kV. Samples: concentration, 0.2 mg/mL in H<sub>2</sub>O; hydrostatic injection, 30 cm, 10 s; detection, 254 nm. The BMA-CNT column used for (A) and (C) was 63.5 cm (58.5 cm) × 75 μm id and was 49.5 cm (44.5 cm) × 75 μm id for (B) and (D). Peak identification in (A) and (C): (1) Cyt; (2) Thy; (3) Gua; (4) Ura; (5) Ade; in (B) and (D): (1) Guo; (2) Cyd; (3) Thd; (4) Urd; (5) Ado.

course, other factors affecting electrophoretic mobility or  $k'_e$  values, such as Stokes radius and ion–ion interactions with the borate buffer, should be considered [48, 49].

Ade and Ado had the highest retention factor ( $k''$ ) values among the nucleobases and nucleosides, respectively. These two solutes are built from purine units and consist of nitrogen heterocycles with a double ring that creates an enhancement of the  $\pi$ – $\pi$  interaction with the carbon double bonds in the MWNT structure. Although Gua and Guo also contain purine moieties, they did not have high  $k''$  values, suggesting that in addition to the  $\pi$ – $\pi$  interaction, other interactions, such as hydrogen bonding, Van der Waals forces and electrostatic interactions contribute to the chromatographic retention. In fact, the electrostatic repulsion between anionic solutes and carboxylate groups on the modified MWNTs would dominate the retention of some solutes with negative  $k''$  values. Regardless of the extent of each interaction, a reverse-phase mechanism could be proved through the addition of an organic modifier to the running buffer. As expected, the  $k''$  values were decreased as MeOH concentration was increased for nucleobases, as shown in Fig. 6(A). For nucleosides, however, the plots of  $k''$  values against the ACN volume ratios present the concave curves with maxima around 10% ACN, as shown in Fig. 6(B). This phenomenon could be attributed to the increase in  $pK_a$  values as the percentage of organic modifier increased in the running buffer and more neutral solutes were formed and retained. Addition of ACN tends to increase  $pK_a$  values more than MeOH does [50]. As more than 10% of ACN was added, the  $k''$  values were decreased by the reverse-phase mechanism.

Overall, neither electrophoresis nor chromatography predominated over CEC separations of nucleobases, that is, the two mechanisms collectively determined the migration order. For nucleosides, chromatography seemed to take a major role in the determination of migration order, which could be due to the large contribution of deoxyribose to chromatographic retention.

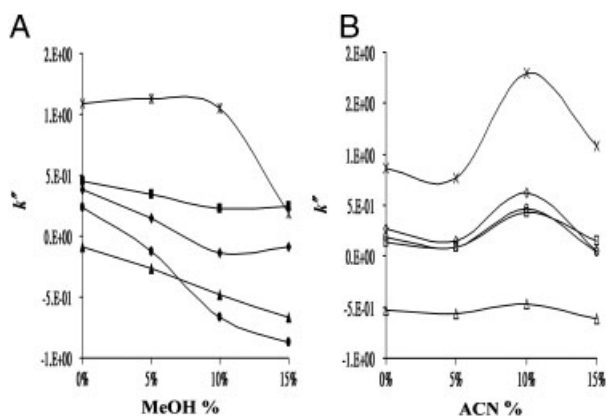
### 3.3 Separation of flavonoids

In comparison with nucleobases and nucleosides, flavonoids are less polar and probably require some organic modifiers added to the running buffer. The flavonoids, one class of polyphenols, had been separated in our previous studies using silica-hydride monolayer, and polyacrylate-modified capillaries [28, 41]. According to the previous reports, neither the hydride-based capillaries nor the polymer-based capillaries were capable of base-line separations of flavonoids without the addition of MeOH to the buffers. In this study, the BMA-CNT capillary also could not separate these flavonoids without the addition of an organic modifier. The presence of an organic modifier not only altered the EOF, but it also affected the chromatographic partitioning between the flavonoid molecules and the modified surfaces of these capillaries. Optimization of this factor is necessary for the CEC separation of flavonoids.

After systematic trials, the optimum BGE for the selected flavonoids in the BMA-CNT column seemed to be a borate buffer, pH 9.5, 10 mM, mixed with ACN. The effect of various volume ratios of ACN (40, 50, and 60%) on electrochromatograms is demonstrated in Fig. 7. Some, but

**Table 1.** Electrochromatographic parameters of various samples in borate buffers

Migration order	Compounds	$t_{M2}$ (min)	$k'_e$	$k''$	Peak width (s)	Plate numbers ( $\times 10^4$ )	Resolution
Nucleobases separated using the conditions shown in Fig. 5(C)							
1	Cytosine	14.533	-0.63	-0.48	57.237	0.37	3.886
2	Thymine	17.463	-0.28	0.22	33.248	1.6	1.325
3	Guanine	17.905	-0.81	-0.67	6.772	40	13.286
4	Uracil	21.852	-0.59	-0.14	28.879	3.3	20.270
5	Adenine	31.42	-0.33	1.05	27.764	7.4	
Nucleosides separated using the conditions shown in Fig. 5(D)							
1	Guanosine	5.909	-0.53	-0.47	25.354	0.31	13.883
2	Cytidine	10.819	-0.30	0.43	17.088	2.3	5.275
3	Thymidine	12.348	-0.37	0.47	17.696	2.8	8.412
4	Uridine	15.279	-0.44	0.62	24.115	2.3	10.962
5	Adenosine	20.923	-0.29	1.8	37.671	1.8	
Flavonoids separated using the conditions shown in Fig. 7(B)							
1	5-Methoxyflavone	7.636	-0.04	0.53	32.505	0.31	3.2
2	Hesperidin	8.969	-0.11	0.68	17.557	1.5	1.8
3	Naringin	9.474	-0.07	0.85	15.500	2.2	14
4	Epicatechin	14.765	-0.38	0.93	28.578	1.5	2.5
5	Hesperetin	15.743	-0.45	0.81	18.381	4.2	1.9
6	Daidzein	16.334	-0.43	0.95	19.899	3.9	2.8
7	Naringenin	17.283	-0.46	0.94	21.003	3.9	140
8	Quercetin	52.892	-0.46	4.96	9.855	160	
Phenolic acids separated using the conditions shown in Fig. 9(B)							
1	Ethylvanillin	14.71	-0.43	1.31	18.174	3.8	10
2	Chlorogenic acid	18.034	-0.58	1.80	20.978	4.3	4.4
3	Ferulic acid	19.873	-0.64	1.69	29.650	2.6	1.7
4	Syringic acid	20.795	-0.64	1.80	35.092	2.0	5.7
5	<i>p</i> -Coumaric acid	24.49	-0.67	1.98	42.450	1.9	1.2
6	Vanillic acid	25.446	-0.70	1.84	52.458	1.4	6.4
7	<i>p</i> -Hydroxybenzoic acid	32.858	-0.76	1.95	85.521	0.85	4.5
8	Caffeic acid	38.779	-0.85	1.10	71.312	1.7	3.7
9	Gallic acid	44.857	-0.92	0.41	124.577	0.75	5.3
10	Protocatechuic acid	62.498	-0.88	1.80	272.695	0.30	

**Figure 6.** Effect of the addition of MeOH and ACN to the running buffer on the retention factor ( $k''$ ) of (A) nucleobases and (B) nucleotides, respectively, in the BMA-CNT capillary. The CEC conditions are based on those in Fig. 5.

not all, of peaks increased their migration times with an increase in the modifier percentages. This behavior can be explained because the EOF reached a minimum near 40–60% ACN, as shown in Fig. 5. Among the three ratios, 50%

obviously achieved better resolution among the flavonoids, as shown in Fig. 7(B), the electrochromatographic parameters of which are listed in Table 1. Other conditions, such as changes in pH level (pH 8.5 and pH 10.5), concentration (30 mM), and MeOH (50%) were also tried. However, these trial conditions were not comparable to those shown in Fig. 7(B).

In Table 1, both the  $k'_e$  and  $k''$  values are generally parallel to the migration order, that is, the electrophoretic and chromatographic modes collaboratively determined the CEC mechanism. In fact, according to the  $k'_e$  values, flavonoids could be easily divided into two categories. Due to the weakly charged hydroxyl group in 5-methoxyflavone's enol form and the large size of the glucoside moiety in the hesperidin and naringin structures, these three compounds had smaller negative  $k'_e$  values than the other five flavonoids. Even though, a high volume of ACN was added to the BGE, flavonoids have higher  $k''$  values than nucleobases and nucleosides, except for Ade and Ado. The benzo rings in the flavonoid structures might exert stronger  $\pi$ - $\pi$  interactions with the BMA-CNT phase. However, hydrogen bonding did not seem to be a crucial factor as the many hydroxyl groups

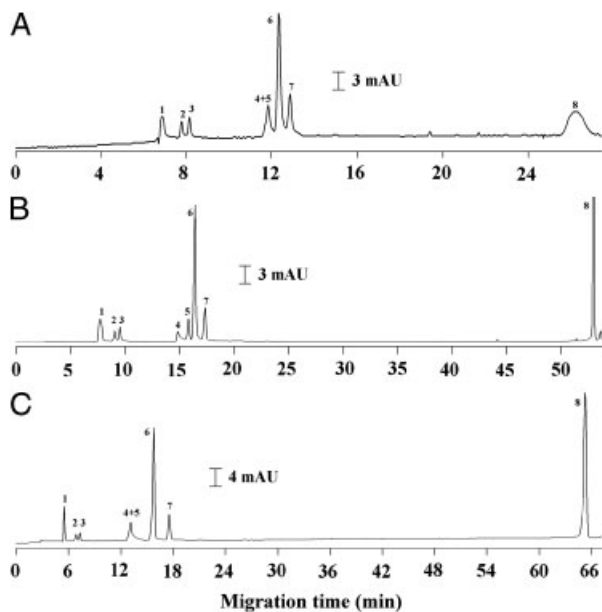


**Figure 7.** Electrochromatographic separations of flavonoids using a BMA-CNT capillary (37.7 cm (32.7 cm)  $\times$  75  $\mu$ m id) with various volume ratios of ACN added in the BGE. (A) 40%; (B) 50%; (C) 60% of ACN added in the borate buffer, 10 mM, pH 9.5. Applied voltage: 10 kV. Samples: concentration, 0.25 mg/mL in MeOH, except epicatechin, hesperetin, and naringenin, which are 0.5 mg/mL in MeOH; hydrostatic injection, 15 cm, 5 s; detection, 280 nm. Peak assignments: (1) 5-methoxyflavone; (2) hesperidin; (3) naringin; (4) epicatechin; (5) hesperetin; (6) daidzein; (7) naringenin; (8) quercetin.

in the hesperidin and naringin structures did not significantly raise their  $k'$  values.

### 3.4 Separation of phenolic acids

In comparison with the above samples, phenolic acids are fully ionized solutes in a general buffer with a moderate pH level. With  $pK_a$  values ranging between 3.59 and 4.64 (chlorogenic, 3.59 [51]; caffeic, 4.04 [52]; protocatechuic, 4.26 [53]; syringic, 4.33 [52]; gallic, 4.41 [53]; ferulic, 4.44 [54]; vanillic acid, 4.51 [53]; *p*-hydroxybenzoic, 4.58 [55]; and *p*-coumaric, 4.64 [51]), the nine phenolic acids were mixed with ethylvanillin,  $pK_a = 7.6$  [56], to be the test sample. With the aid of the cathodic EOF generated by a small voltage of +7 kV, the elution of the acids could be achieved within 21 min using the BMA-CNT capillary in a borate buffer at pH 9.0, as shown in Fig. 8(A). Although the range of  $pK_a$  values of these acids was narrow, a satisfactory selectivity was achieved by the pH 9.5 buffer within 30 min, as shown in Fig. 8(B). However, an attempt to resolve peaks 3 and 4, ferulic acid and syringic acid, by raising the pH level to 10.0 was not successful and resulted in poorer separation, as shown in Fig. 8(C). These separations were very sensitive to changes in pH. If 5% MeOH was added to the pH 9.5 borate buffer, the resolution between peaks 3 and 4 improved, as shown in Fig. 9(A). When 5% ACN or 10% MeOH was used

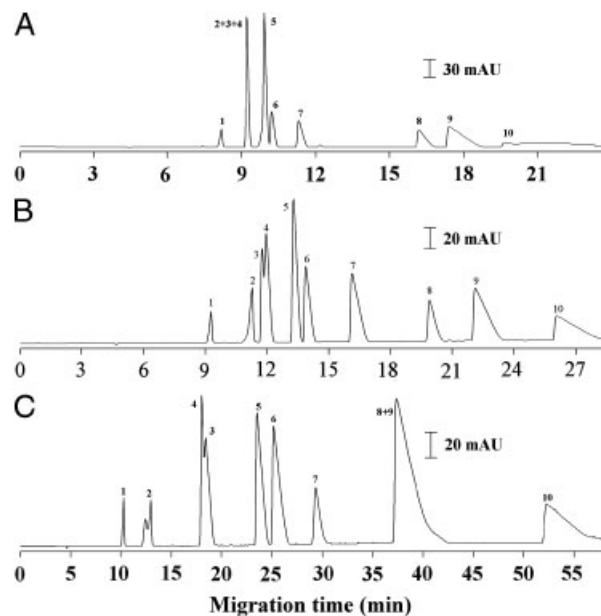


**Figure 8.** Electrochromatographic separations of phenolic acids at different pH values in the BMA-CNT capillary (36 cm (31 cm)  $\times$  75  $\mu$ m id). Conditions: sample concentration, 0.1 M in H<sub>2</sub>O; hydrostatic injection, 15 cm, 1 s; applied voltage, 7 kV; detection, 280 nm; BGE, borate buffer, 30 mM, (A) pH 9.0; (B) pH 9.5; (C) pH 10.0. Peak assignments: (1) ethylvanillin, (2) chlorogenic acid, (3) ferulic acid, (4) syringic acid, (5) *p*-coumaric acid, (6) vanillic acid, (7) 4-hydroxybenzoic acid, (8) caffeic acid, (9) gallic acid, (10) protocatechuic acid.

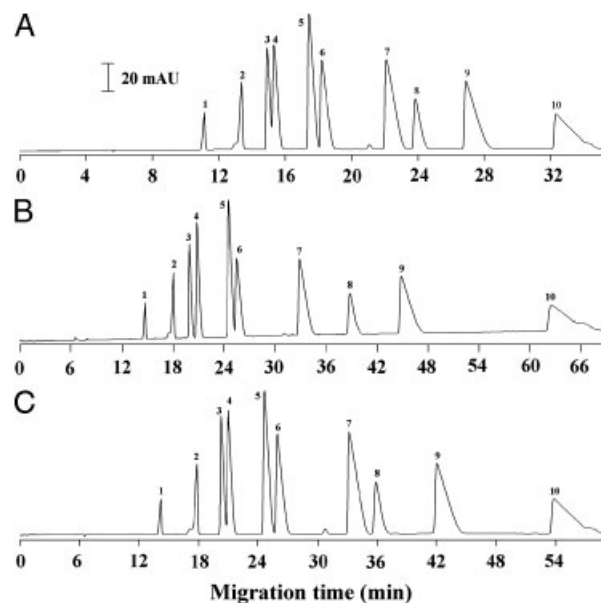


**Figure 9.** Electrochromatographic separations of phenolic acids at various ratios of organic modifier. (A) MeOH, 5% (v/v); (B) MeOH, 10% (v/v); (C) ACN, 5% (v/v) added in the borate buffer, 30 mM, pH 9.0. Other CEC conditions and peak assignments are the same as in Fig. 8(B).



instead, both acids had well-resolved peaks, but prolonged analysis times, as shown, respectively, in Fig. 9(B, C). Besides, some peaks with higher migration orders appear tailings as shown in Figs. 8 and 9. The cause of the peak tailings could reside in sample overloading, extended migration times for anions travelling to cathode, and slow mass transfer through the BMA-CNT phases. Problems arising from the modified phase could be improved by adjusting the ratios of the polymerization constituents and the recipe of wall coating.

The electrochromatographic parameters obtained from Fig. 9(B) are listed in Table 1. Here the  $k'_e$  factor seemed to be the main determinant of the migration order as the values of  $k'_e$  are more closely related to the migration order than  $k''$ . Although the chromatography did not participate in the selectivity significantly, the BMA-CNT phase still strongly retained the acids with positive  $k''$  values.

#### 4 Concluding remarks

As characterized by ATR-IR and SEM, MWNT materials with highly reactive cyclopentadienyl carbon atoms in the CNT structure were successfully copolymerized with BMA to form a BMA-CNT phase on a capillary wall. The carboxylate groups on the acid-treated MWNTs created a double layer on the BMA-CNT phase surface and demonstrated unique EOF profiles that changed with the pH of the running buffers. Four kinds of samples, including nucleobases, nucleosides, flavonoids, and phenolic acids, with various ionic and polar properties were well separated by optimizing the CEC conditions and were also used to probe the CEC mechanism. By calculating the velocity and retention factors from the electrochromatograms, electrophoretic and chromatographic contributions to the CEC performance could be independently evaluated. Several solute stationary phase interactions, such as  $\pi$ - $\pi$  interaction, electrostatic repulsion, and hydrogen bonding, were surmised to influence the chromatographic retention of these samples. Furthermore, a reversed-phase chromatographic mode was identified by addition of organic modifier into running buffers. In the future, studies on the incorporation of CNTs into silica-based and polymeric matrices, such as polyacrylamides and polystyrene, will be continued.

Support of this work by the National Science Council of Taiwan is gratefully acknowledged (NSC-98-2113-M-039-003-MY3).

The authors have declared no conflict of interest.

#### 5 References

[1] Ou, J., Dong, J., Dong, X., Yu, Z., Ye, M., Zou, H., *Electrophoresis* 2007, 28, 148–163.

- [2] Dong, X., Wu, R., Dong, J., Wu, M., Zhu, Y., Zou, H., *Electrophoresis* 2009, 30, 141–154.
- [3] Pesek, J. J., Matyska, M. T., Salgotra, V., *Electrophoresis* 2008, 29, 3842–3849.
- [4] Yin, X.-B., Liu, D.-Y., *J. Chromatogr. A* 2008, 1212, 130–136.
- [5] Xu, L., Dong, X.-Y., Sun, Y., *Electrophoresis* 2009, 30, 689–695.
- [6] Tian, Y., Li, H., Zeng, Z., *Electrophoresis* 2006, 27, 3381–3390.
- [7] Liu, C.-Y., Chen, T.-H., Misra, T. K., *J. Chromatogr. A* 2007, 1154, 407–415.
- [8] Chen, J.-L., *Electrophoresis* 2006, 27, 729–735.
- [9] Xu, L., Dong, X.-Y., Sun, Y., *Electrophoresis* 2009, 30, 689–695.
- [10] Nilsson, C., Birnbaum, S., Nilsson, S., *J. Chromatogr. A* 2007, 1168, 212–224.
- [11] Zhang, S., Macka, M., Haddad, P. R., *Electrophoresis* 2006, 27, 1069–1077.
- [12] Ruiz-Jiménez, J., Kuldvee, R., Chen, J., Öörni, K., Kovanen, P., Riekkola, M. -L., *Electrophoresis* 2007, 28, 779–788.
- [13] Vainikka, K., Chen, J., Metso, J., Jauhiainen, M., Riekkola, M.-L., *Electrophoresis* 2007, 28, 2267–2274.
- [14] Huang, Y.-F., Chiang, C.-K., Lin, Y.-W., Liu, K., Hu, C.-C., Bair, M.-J., Chang, H.-T., *Electrophoresis* 2008, 29, 1942–1951.
- [15] Dong, X., Wu, R., Dong, J., Wu, M., Zhu, Y., Zou, H., *Electrophoresis* 2008, 29, 3933–3940.
- [16] Hsieh, Y.-L., Chen, T.-H., Liu, C.-P., Liu, C.-Y., *Electrophoresis* 2005, 26, 4089–4097.
- [17] Li, T., Xu, Y., Feng, Y.-Q., *J. Liq. Chromatogr. Relat. Technol.* 2009, 32, 2484–2498.
- [18] Yang, L., Guihen, E., Holmes, J. D., Loughran, M., O'Sullivan, G. P., Glennon, J. D., *Anal. Chem.* 2005, 77, 1840–1846.
- [19] Li, H.-F., Zeng, H., Chen, Z., Lin, J.-M., *Electrophoresis* 2009, 30, 1022–1029.
- [20] Qu, Q., Zhang, X., Shen, M., Liu, Y., Hu, X., Yang, G., Wang, C., Zhang, Y., Yan, C., *Electrophoresis* 2008, 29, 901–909.
- [21] Luong, J. H. T., Bouvrette, P., Liu, Y., Yang, D.-Q., Sacher, E., *J. Chromatogr. A* 2005, 1074, 187–194.
- [22] Li, Y., Chen, Y., Xiang, R., Ciuparu, D., Pfefferle, L. D., Horváth, C., Wilkins, J. A., *Anal. Chem.* 2005, 77, 1398–1406.
- [23] Weng, X., Bi, H., Liu, B., Kong, J., *Electrophoresis* 2006, 27, 3129–3135.
- [24] Sombra, L., Moliner-Martínez, Y., Cárdenas, S., Valcárcel, M., *Electrophoresis* 2008, 29, 3850–3857.
- [25] Chen, J.-L., *J. Chromatogr. A* 2010, 1217, 715–721.
- [26] Jia, Z., Wang, Z., Xu, C., Liang, J., Wei, B., Wu, D., Zhu, S., *Mater. Sci. Eng. A* 1999, 271, 395–400.
- [27] Park, S. J., Cho, M. S., Lim, S. T., Choi, H. J., Jhon, M. S., *Macro. Rapid Commun.* 2003, 24, 1070–1073.
- [28] Chen, J.-L., Lin, Y.-C., *J. Chromatogr. A* 2010, 1217, 4328–4336.

- [29] Chuang, S.-C., Chang, C.-Y., Liu, C.-Y., *J. Chromatogr. A* 2004, 1044, 229–236.
- [30] Eeltink, S., Svec, F., Fréchet, J. M. J., *Electrophoresis* 2006, 27, 4249–4256.
- [31] Zaidi, S. A., Cheong, W. J., *J. Chromatogr. A* 2009, 1216, 2947–2952.
- [32] Silverstein, R. M., Webster, F. X., Kiemle, D., *Spectrometric Identification of Organic Compounds*, 7th Edn, John Wiley & Sons, New Jersey 2005.
- [33] Kang, X., Ma, W., Zhang, H.-L., Xu, Z.-G., Guo, Y., Xiong, Y., *J. Appl. Polym. Sci.* 2008, 110, 1915–1920.
- [34] Sombra, L., Moliner-Martínez, Y., Cárdenas, S., Valcárcel, M., *Electrophoresis* 2008, 29, 3850–3857.
- [35] Zou, W., Du, Z.-j., Liu, Y.-x., Yang, X., Li, H.-q., Zhang, C., *Compos. Sci. Technol.* 2008, 68, 3259–3264.
- [36] Liu, J., Rinzler, A. G., Dai, H., Hafner, J. H., Bradley, R. K., Boul, P. J., Lu, A., Iverson, T., Shelimov, K., Huffman, C. B., Rodriguez-Macias, F., Shon, Y. -S., Lee, T. R., Colbert, D. T., Smalley, R. E., *Science* 1998, 280, 1253–1256.
- [37] Jankowska, H., Swiatkowski, A., Choma, J., *Active Carbon*, Ellis Horwood, New York 1991.
- [38] Attard, P., Antelmi, D., Larson, I., *Langmuir* 2000, 16, 1542–1552.
- [39] Thabano, J. R. E., Breadmore, M. C., Hutchinson, J. P., Johns, C., Haddad, P. R., *J. Chromatogr. A* 2007, 1175, 117–126.
- [40] Chen, J.-L., *Electrophoresis* 2009, 30, 3855–3862.
- [41] Chen, J.-L., *J. Chromatogr. A* 2009, 1216, 6236–6244.
- [42] Schmitt-Kopplin, P., Hertkorn, N., Garrison, A. W., Freitag, D., Kettrup, A., *Anal. Chem.* 1998, 70, 3798–3808.
- [43] Haunschmidt, M., Buchberger, W., Klampfl, C. W., *J. Chromatogr. A* 2008, 1213, 88–92.
- [44] Rathore, A. S., Horváth, C., *J. Chromatogr. A* 1996, 743, 231–246.
- [45] Rathore, A. S., Horváth, C., *Electrophoresis* 2002, 23, 1211–1216.
- [46] Furumoto, T., Fukumoto, T., Sekiguchi, M., Sugiyama, T., Watarai, H., *Electrophoresis* 2001, 22, 3438–3443.
- [47] Geldart, S. E., Brown, P. R., *J. Chromatogr. A* 1999, 831, 123–129.
- [48] Porras, S. P., Riekkola, M.-L., Kenndler, E., *J. Chromatogr. A* 2001, 924, 31–42.
- [49] Haunschmidt, M., Buchberger, W., Klampfl, C. W., *J. Chromatogr. A* 2008, 1213, 88–92.
- [50] Porras, S. P., Kenndler, E., *J. Chromatogr. A* 2004, 1037, 455–465.
- [51] Serjeant, E. P., Dempsey, B., *Ionization Constants of Organic Acids in Aqueous Solution IUPAC Chemical Data Series No.23*, Pergamon Press, Oxford 1979.
- [52] Huang, H.-Y., Lien, W.-C., Huang, I.-Y., *Electrophoresis* 2006, 27, 3202–3209.
- [53] Dawson, R. M. C., Elliott, D. C., Elliott, W. H., Jones, K. M., *Data for Biochemical Research*, Oxford Science Publications, Oxford 1986.
- [54] Maegawa, Y., Sugino, K., Sakurai, H., *Free Radic. Res.* 2007, 41, 110–119.
- [55] Martell, A. E., Smith, R. M., *Critical Stability Constants*, Plenum Press, New York 1974.
- [56] Lavine, B. K., Hendayana, S., Cooper, W. T., He, Y., *J. Liq. Chrom. Relat. Technol.* 1997, 20, 377–402.